Fingerprint Warping Using Ridge Curve Correspondences

Arun Ross, *Member*, *IEEE*, Sarat C. Dass, and Anil K. Jain, *Fellow*, *IEEE*

Abstract—The performance of a fingerprint matching system is affected by the nonlinear deformation introduced in the fingerprint impression during image acquisition. This nonlinear deformation causes fingerprint features such as minutiae points and ridge curves to be distorted in a complex manner. A technique is presented to estimate the nonlinear distortion in fingerprint pairs based on ridge curve correspondences. The nonlinear distortion, represented using the thin-plate spline (TPS) function, aids in the estimation of an "average" deformation model for a specific finger when several impressions of that finger are available. The estimated average deformation is then utilized to distort the template fingerprint prior to matching it with an input fingerprint. The proposed deformation model based on ridge curves leads to a better alignment of two fingerprint images compared to a deformation model based on minutiae patterns. An index of deformation is proposed for selecting the "optimal" deformation model arising from multiple impressions associated with a finger. Results based on experimental data consisting of 1,600 fingerprints corresponding to 50 different fingers collected over a period of two weeks show that incorporating the proposed deformation model results in an improvement in the matching performance.

Index Terms—Fingerprints, nonlinear deformation, ridge curves, thin plate spline, index of deformation, minutiae pattern, template selection.

1 Introduction

The uniqueness of a fingerprint is dictated by the topographic relief of its ridge structure and the presence of ridge anomalies, termed minutiae points. The problem of automatic fingerprint matching involves determining the degree of similarity between two fingerprint impressions by comparing their ridge structure and the spatial distribution of the minutiae points [2], [3], [4], [5]. However, the image acquisition process introduces nonlinear distortions in the ridge structure due to the nonuniform finger pressure applied by the subject and the elastic nature of the skin. The effects of these nonlinear distortions must be addressed when matching two fingerprint images. Models based on affine transformations invariably lead to unsatisfactory matching results since the distortions are basically elastic (nonrigid) in nature (Fig. 1).

To deal with the problem of nonlinear distortion in fingerprint images, four types of approaches have been discussed in the literature. The first approach accounts for distortion in the image *acquisition* stage by capturing the least distorted print from the user while rejecting the others. Ratha and Bolle [6] describe a system which does not accept a fingerprint image if the user applies excessive force on the sensor. The system operates by measuring the forces and torques applied on the sensor. Dorai et al. [7] observe a video sequence of the fingertip as it interacts with the sensor and measure the distortion across successive frames. When excessive distortion is observed, the system requests the user to provide another fingerprint. These systems require specialized hardware and the ability to perform extensive computations in real-time. As a result, they do not offer a practical solution to fingerprint deformation in real-time embedded fingerprint applications.

In the second approach, the distortion is estimated during the *matching* stage. Thebaud [8] uses a gradient descent technique to compute local warps when comparing two fingerprints. The fingerprint correlation score is used as the objective function. Besides being time consuming, this technique potentially results in a higher False Accept Rate (FAR) since it performs local warping to force a match between the two images. Kovács-Vajna [4] uses minutiae triplets to compare two minutiae sets. By not using the entire minutiae pattern at once, the cumulative effect of distortion is avoided. Bazen and Gerez [9] use a thin-plate spline (TPS) model to account for nonlinear distortions when comparing two minutiae sets.

In the third approach, the distortion is removed *before* the matching stage. Senior and Bolle [10] have developed a model which assumes that ridges in a fingerprint are constantly spaced and that deviations from this model indicate the presence of elastic distortions. They apply local warps in regions exhibiting such deviations so that local ridge distances nearly equal the average interridge spacing. Their experimental results show a significant improvement in genuine matching scores (i.e., the matching score when comparing two impressions of the same finger), as indicated by the t-statistic. However, their assumption that interridge spacing in a fingerprint is a constant is not always valid. Watson et al. [11] construct distortion tolerant filters for each (template) fingerprint. These filters when applied to the image before matching are shown to result in improved system performance.

The fourth approach is more suited for introducing distortions in synthetic fingerprints. Cappelli et al. [12] have

- *A. Ross is with the Lane Department of Computer Science and Electrical Engineering, West Virginia University, PO Box 6109, Morgantown, WV 26506. E-mail: arun.ross@mail.wvu.edu.*
- *S.C. Dass is with the Department of Statistics, Michigan State University, A-439 Wells Hall, East Lansing, MI 48824. E-mail: sdass@stt.msu.edu.*
- *A.K. Jain is with the Department of Computer Science and Engineering, Michigan State University, 3115 Engineering Building, East Lansing, MI 48824. E-mail: jain@cse.msu.edu.*

Manuscript received 4 Sept. 2003; revised 6 Apr. 2005; accepted 7 Apr. 2005; published online 11 Nov. 2005.
Recommended for acceptance by K. Yamamoto.
For information on obtaining reprints of this article, please send e-mail to: tpami@computer.org, and reference IEEECS Log Number TPAMI-0260-0903.

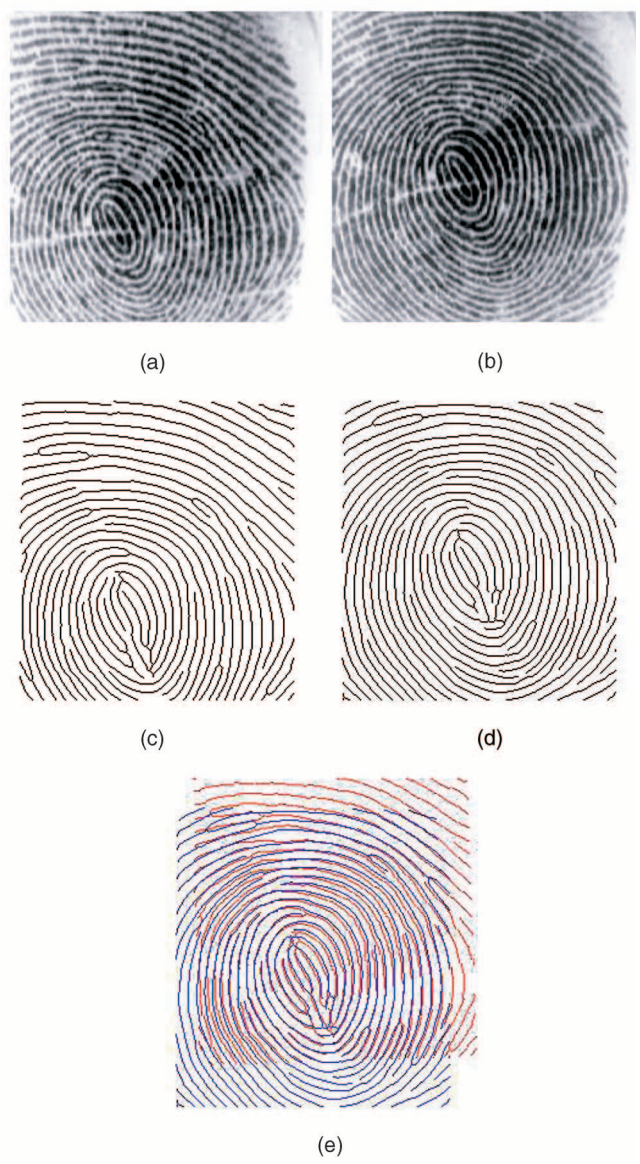

Fig. 1. Alignment of two impressions of the same finger using affine transformation. (a) and (b) are the gray-scale images, (c) and (d) are the thinned (skeletonized) images of (a) and (b), respectively, and (e) shows the alignment based on the thinned images. Ridge lines do not align in (e).

attempted to model the distortions that could occur in a fingerprint image by considering three concentric regions in a fingerprint; the inner and outer regions are assumed to have no distortions although ridges in the outer region can be translated and rotated with respect to the ridges in the inner region; the region in between is assumed to undergo nonlinear distortions in order to accommodate the transition of ridges from the inner to the outer region. The authors, however, do not use this model to perform fingerprint matching. Rather, they use it to synthesize multiple impressions of the same finger [13].

Most current techniques deal with the problem of nonlinear distortion on a case by case basis, i.e., for *every* pair of fingerprint impressions (or for every fingerprint impression), a distortion removal technique is applied and a matching score generated. No attempt has been made thus far to develop a *finger-specific deformation model* that can be computed offline and later used for matching. The advantage of such a scheme is that, once a finger-specific model has been computed and stored along with the template, recomputation of the model is not necessary during matching. In this paper, we propose a technique for computing the *average* deformation model of a fingerprint impression by using the thin plate spline (TPS) warping model. It is assumed that multiple impressions of a user's fingerprint are available during the training phase. The model is expected to capture the intraclass variability due to nonlinear deformations in a fingerprint impression. The relative distortion between two impressions is estimated based on their ridge curve correspondences. The average deformation model associated with an arbitrary fingerprint impression (called the baseline impression) is an indication of its average distortion with respect to other impressions of the same finger. For a single finger, an optimal baseline impression with the most consistent distortions (i.e., distortions that deviate the least from the average) is selected based on its index of deformation. We demonstrate that predistorting the baseline impression using the average deformation model can improve matching performance.

Earlier work in modeling the nonlinear distortion in fingerprint images [14], [9], [15] used only the spatial distribution of the minutiae points (Fig. 2). In this paper, the relative distortions are estimated based on ridge curve correspondence (Fig. 3). Modeling the distortion using ridge curve correspondences offers several advantages over minutiae correspondences, resulting in improved matching performance. Unlike minutiae points, which can be sparsely distributed in certain regions of a fingerprint image, ridge curves are present all over the image domain, thereby permitting a more reliable estimate of the distortion. The spatial continuity of ridge curves enables sampling of a large number of points on the ridges for establishing correspondences, including points in the vicinity of undetected minutiae points. Also, in some poor quality images, minutiae information cannot be reliably extracted and, thus, cannot be used to construct a fingerprint distortion model. For these reasons, ridge curve-based warping techniques are expected to provide a robust and reliable estimate of the distortion in fingerprint impressions.

The rest of the paper is organized as follows: Section 2 lists a few warping (deformation) models commonly used in the literature and presents the warping model based on thin-plate splines (TPS) that has been used in this work, Section 3 describes the average deformation model that we propose, Section 3.1 defines the index of deformation that is utilized to select the optimal deformation model from a given set of models, Section 4 describes the experiments conducted and the results obtained, and Section 5 summarizes the paper and presents future directions for research.

2 The Fingerprint Warping Model

Warping methods can be used to obtain global deformation models for image registration. Applications of warping techniques abound in the statistical, medical imaging, and computer vision literature. Examples include warping by elastic deformations [16], [17], optical or fluid flow [18], [19], [20], diffusion processes [21], Bayesian prior distributions [22], [23], and thin-plate splines (TPS) [24], [25], [26]. Only recently have warping techniques based on deformation models been used to describe distortions in fingerprint images for the purpose of matching [14], [9]. Bazen and Gerez [9] show that the use of nonlinear deformation models, as opposed to

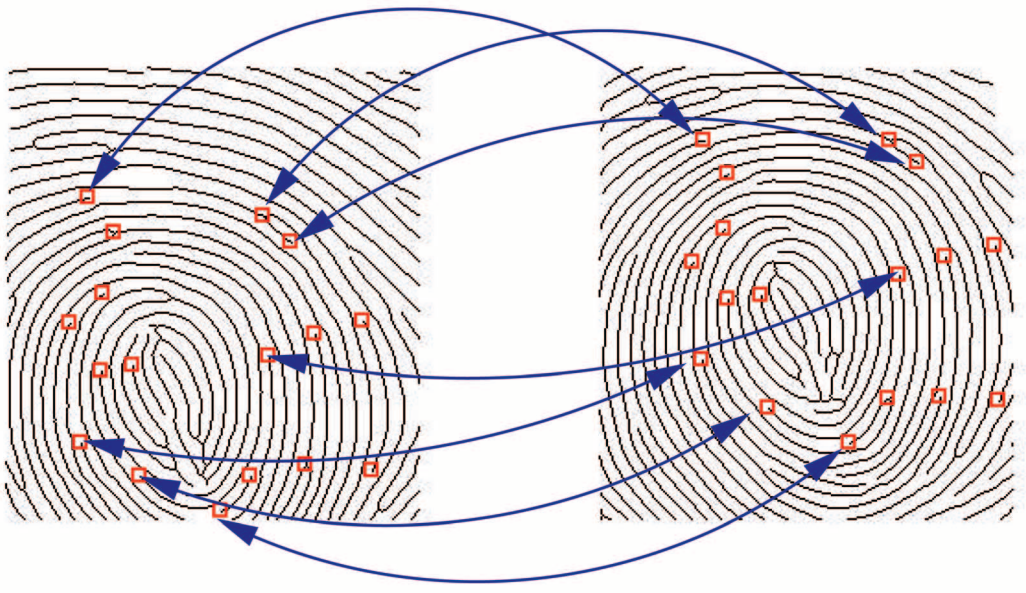

Fig. 2. An example of minutiae correspondences between two impressions of a finger.

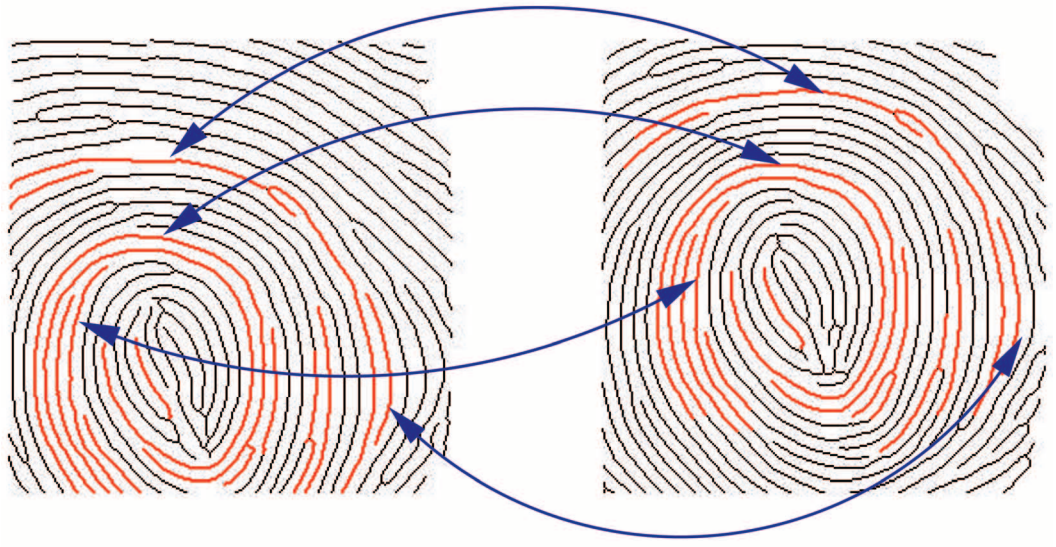

Fig. 3. An example of ridge curve correspondences between two impressions of a finger.

simple rigid transformations, can result in significant improvement in fingerprint matching performance.

In this work, a landmark-based registration scheme is employed. Specifically, we use a skeletonized version of a fingerprint image, known as the thinned image, to extract ridge curve information (see Fig. 1) that is sampled at regular intervals in order to derive landmark points. Estimating the deformation model based on ridge curves offers several advantages over minutiae point patterns. First, ridge lines are distributed over the entire fingerprint image and, thus, a more reliable deformation model can be obtained. Second, the likelihood of incorrectly associating two ridge curves is much less than incorrectly associating two minutiae points due to the richer intrinsic information available in curves compared to points. Consequently, the deformation model based on ridge curves yields better matching performance compared to minutiae points.

When multiple impressions of a finger are available, the relative distortion between one pair can be significantly different from another pair (Fig. 4). Furthermore, even in a single impression, the deformation of the ridges can vary from region to region. Thus, we address the following two problems: 1) Obtain a deformation model based on ridge curve correspondences that can be incorporated in the matching stage and 2) given multiple deformation models for a finger (each model corresponds to one impression of the finger), select the optimal model that has the most consistent distortion effects as measured from a baseline impression.

Let $I_0(x, y)$ and $I_1(x, y)$ denote two fingerprint impressions, where $(x, y) \in S$ for a domain $S \subset R^2$. Our convention is to refer to I_0 and I_1 as the template and query (or input) images, respectively. A warping of I_0 to I_1 is defined as the function $F : S \rightarrow S$ such that

$$F(I_0) = I_1. \tag{1}$$

We register the two impressions I_0 and I_1 by matching corresponding ridge curves. Thus, in (1), the warping function, $F : S \rightarrow S$, registers two sets of ridge curves derived from I_0 and I_1. Let $u_k \equiv u_k(t) = (u_{k1}(t), u_{k2}(t))^T$

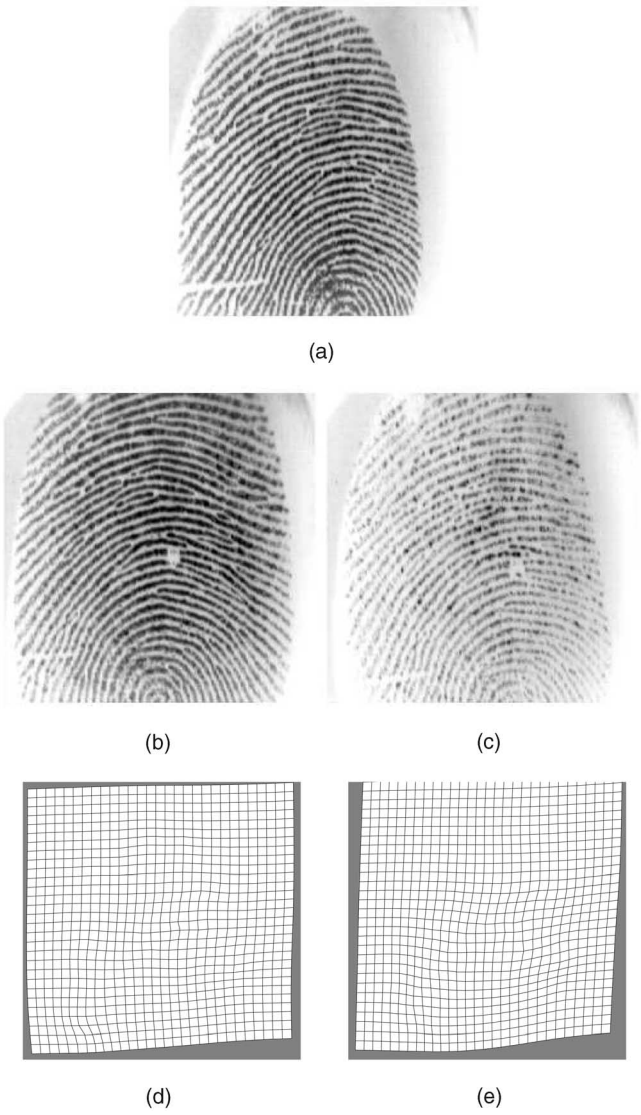

Fig. 4. Nonlinear deformations (with rotation and translation parameters removed) associated with two pairings involving the same template: (a) Template image. (b) and (c) Query images. (d) and (e) Nonlinear deformation of (a) into (b) and (c), respectively.

denote a discretized ridge curve in I_0 for $k = 1, 2, \ldots, n$, and let $v_k \equiv v_k(t) = (v_{k1}(t), v_{k2}(t))^T$, $k = 1, 2, \ldots, n$, denote the corresponding discretized ridge curves in I_1. Here, t is the index of discrete points on a single ridge curve and n is the total number of corresponding curves. The two sets of ridge curves, one set in I_0 and the other in I_1, with known correspondences is denoted by the pair (U, V) where $U = (u_1, u_2, \ldots, u_n)^T$ and $V = (v_1, v_2, \ldots, v_n)^T$. We assume that each correspondence pair is aligned as close as possible using rigid transformation prior to nonlinear warping. This can be achieved using the Procrustes analysis ([27], [28]) after pairs of corresponding points are obtained using the methodology outlined in Section 2.2. For n pairs of ridge curve correspondences, a warping function, F, that warps U to V, subject to perfect alignment, is given by the conditions

$$F(u_k) = v_k \tag{2}$$

for $k = 1, 2, \ldots, n$.

2.1 Establishing Ridge Curve Correspondences

Given a pair of gray-scale fingerprint images, I_0 and I_1, we obtain their thinned versions, R_0 and R_1, using the algorithm described in [29]. A thinned image is a binary image (see Figs. 1c and 1d) with gray-scale values of 0 (indicating ridges) and 255 (indicating valleys). Each thinned image can be thought of as a collection of ridge curves. In order to develop ridge curve correspondences, we proceed as follows:

1. Minutiae points are extracted from I_0 and I_1 using the algorithm described in [29]. Let $M_0 = (m_{0,1}, m_{0,2}, \ldots, m_{0,K_0})$ and $M_1 = (m_{1,1}, m_{1,2}, \ldots, m_{1,K_1})$ denote the two minutiae sets of cardinalities K_0 and K_1, respectively. Here, each minutiae point $m_{i,j}$ is characterized by its location in the image, the orientation of the associated ridge, and the gray-scale intensity of pixels in its vicinity.
2. Minutiae correspondences between M_0 and M_1 is obtained using the elastic string matching technique described in [29]. The output of the matcher is a similarity score in the range [0, 1000] and a set of correspondences of the form $C = \{(m_{0,a_j}, m_{1,b_j}) : j = 1, 2, \ldots, K\}$, where $K \leq \min\{K_0, K_1\}$, and the a_js (b_js) are all distinct. Fig. 2 shows an example of the minutiae point pattern correspondence for two impressions of a finger.
3. Once the correspondence between M_0 and M_1 is established, the ridge curves associated with these minutiae points are extracted from R_0 and R_1 using a simple ridge tracing technique. A minutiae point that is a ridge ending has one ridge curve associated with it, while a ridge bifurcation has three associated ridges. In the case of a ridge ending, the ridge curve correspondence between the two images can be easily established since each minutiae point has only one associated ridge curve. However, in the case of a ridge bifurcation, the problem of establishing ridge curve correspondences is nontrivial due to the presence of multiple ridge curves for each minutiae point; each of the three component ridge curves of one minutiae point can potentially match with any component of the other impression.

   To resolve this ambiguity, each ridge curve corresponding to the minutiae point in I_0 (I_1) is represented as a directional vector r_j (s_j), $j = 1, 2, 3$, based on two points on the ridge curve: the minutiae point and the dth point ($d = 20$) on the ridge from the minutiae (see Fig. 5). We define $\theta_{j,k}$ ($\gamma_{j,k}$) to be the angle that r_j (s_j) makes with r_k (s_k), for $k \neq j$. We find the vector r_j (s_j) for which the angles $\{\theta_{j,k},\ k \neq j\}$ ($\{\gamma_{j,k}, k \neq j\}$) are both obtuse. This establishes the first ridge curve correspondence, say, $r_1 \sim s_1$, without loss of generality. We then compute the cross products $c_r = r_2 \times r_3$ and $c_s = s_2 \times s_3$. We assign the correspondence $r_2 \sim s_2$ and $r_3 \sim s_3$ if c_r and c_s are of the same sign and $r_2 \sim s_3$ and $r_3 \sim s_2$, otherwise. Fig. 3 shows an example of ridge curve correspondence for a pair of impressions of a finger.

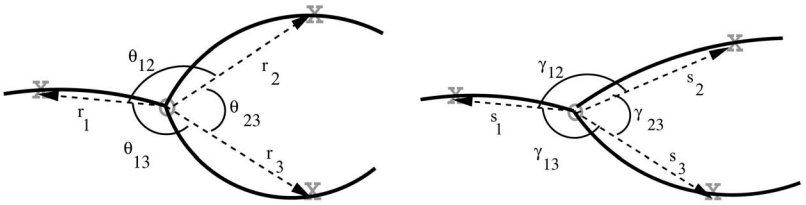

Fig. 5. Vector representation of ridge bifurcation used to establish correspondences between component ridge curves. O marks the bifurcation points in correspondence and X marks the points on the ridges at Euclidean distance d from O.

2.2 Sampling Ridge Curves

Having determined the corresponding ridge curves, we next establish a correspondence between *points* on these curves by sampling every qth point ($q = 20$) on each of the ridge curves. For the correspondence pair (U, V), we have $u_k \equiv u_k(t)$ and $v_k \equiv v_k(t)$ for $k = 1, 2, \ldots, n$. The sampling of the kth corresponding ridge curves, say at points $t_1, t_2, \ldots, t_{g_k}$, yields g_k pairings of the form $(u_k(t_j), v_k(t_j))$ for $j = 1, 2, \ldots, g_k$. Thus, we have a total of $N = \sum_{k=1}^{n} g_k$ points in establishing the correspondence. We denote this set of corresponding points by $\mathcal{U} = (u_1^*, u_2^*, \ldots, u_N^*)^T$ and $\mathcal{V} = (v_1^*, v_2^*, \ldots, v_N^*)^T$. We use TPS to estimate the nonlinear deformation F based on these points. TPS represents a natural parametric generalization from rigid to mild nonrigid deformations. The deformation model for TPS is given in terms of the warping function $F(u)$, with

$$F(u) = c + A \cdot u + W^T s(u), \tag{3}$$

where $u \in S$, c is a 2×1 translation vector, A is a 2×2 affine matrix, W is a $N \times 2$ coefficient matrix, $s(u) = (\sigma(u - u_1^*), \sigma(u - u_2^*), \ldots, \sigma(u - u_N^*))^T$, where

$$\sigma(u) = \begin{cases} ||u||^2 \log(||u||), & ||u|| > 0 \\ 0, & ||u|| = 0. \end{cases} \tag{4}$$

In (3), there are 6 and $2N$ parameters corresponding to the rigid and nonrigid parts of the deformation model, respectively, resulting in a total of $2N + 6$ parameters to be estimated. The restrictions

$$F(u_j^*) = v_j^*, \tag{5}$$

$j = 1, 2, \ldots, N$, provide $2N$ constraints. For the parameters to be uniquely estimated, we further assume that W satisfies the two conditions: 1) $1_N^T W = 0$ and 2) $U_s^T W = 0$, where 1_N is the vector of ones of length N. Thus, the parameters of the TPS model can be obtained from the matrix equation

$$\begin{bmatrix} H & 1_N & \mathcal{U} \\ 1_N^T & 0 & 0 \\ \mathcal{U}^T & 0 & 0 \end{bmatrix} \begin{bmatrix} W \\ c^T \\ A^T \end{bmatrix} = \begin{bmatrix} \mathcal{V} \\ 0 \\ 0 \end{bmatrix}, \tag{6}$$

where H is the $N \times N$ matrix with entries $h_{ij} = \sigma(u_i^* - u_j^*)$.

The matrix in (6) gives rise to a TPS model that minimizes the bending energy subject to the perfect alignment constraints in (5). A more robust TPS model can be obtained by relaxing the constraints in (5) and instead determining the function F which minimizes the expression

$$\sum_{j=1}^{N} \left(v_j^* - F(u_j^*)\right)^T (v_j^* - F(u_j^*)) + \lambda J(F), \tag{7}$$

where

$$J(F) = \sum_{j=1}^{2} \int_S \left\{ \left(\frac{\partial^2 F_j(x,y)}{\partial x^2} \right)^2 + 2 \left(\frac{\partial^2 F_j(x,y)}{\partial x \partial y} \right)^2 + \left(\frac{\partial^2 F_j(x,y)}{\partial y^2} \right)^2 \right\} dx\, dy \tag{8}$$

represents the bending energy associated with $F = (F_1, F_2)^T$, F_j is the jth component of F, and $\lambda > 0$. The case $\lambda = 0$ gives rise to the TPS model described by (6). For general $\lambda > 0$, the parameters of the resulting TPS model can be obtained using (6) with H replaced by $H + \lambda I_N$, where I_N is the $N \times N$ Identity matrix.

3 Average Deformation Model

Suppose we have L impressions of a finger, $T_1, T_2, \ldots, T_L$. Each impression, T_i, can be paired with the remaining impressions, $T_j, j \neq i$, to create $L - 1$ pairs of the form (T_i, T_j). For the pair (T_i, T_j), we obtain a nonlinear transformation F_{ij} by employing the technique described in Section 2. Note that F_{ij} transforms *every* pixel in the template fingerprint, T_i, to a new location. Thus, we can compute the *average* deformation of each pixel u in T_i as

$$\bar{F}_i(u) = \frac{1}{L-1} \sum_{j \neq i} F_{ij}(u). \tag{9}$$

There will be L average deformation models corresponding to the L impressions of the finger. The average deformation is the typical deformation that arises when we compare one fingerprint impression of a finger (the baseline impression) with other impressions of the same finger. Fig. 6 shows that changing the baseline impression for the finger will result in a different average deformation model for that finger (the Φ values are as discussed in Section 3.1). Fig. 7 shows the average deformation for three different fingers; it can be clearly seen that the average warping functions are different for the three fingers, indicating that the fingerprint deformation is finger-specific.

3.1 The Φ Index of Deformation

We consider the following two questions in this section:

1. Which of the L average deformation models can be considered to be the optimal model for this finger?

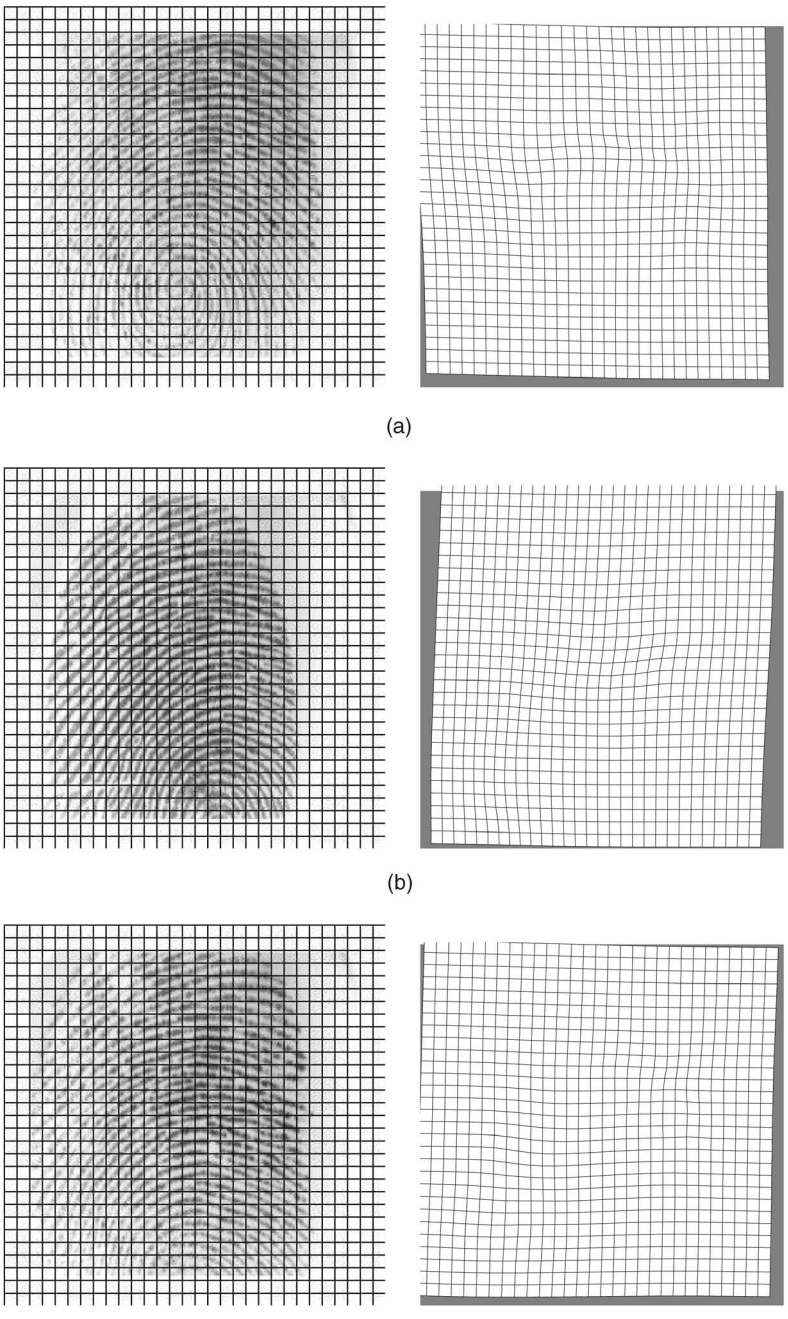

Fig. 6a. The average deformation model (shown as deformations on a reference grid) corresponding to six templates of a finger sorted in increasing Φ-values. (a) is chosen to be the optimal template since it has the least Φ-value. (a) $\Phi = 15.54$. (b) $\Phi = 17.97$. (c) $\Phi = 48.79$.

2. Will the optimal model, when incorporated in the matching stage, result in improved performance compared to the suboptimal models?

In order to address these questions, we first define the pixel-wise covariance matrix associated with the ith average deformation, $\bar{F}_i$, as follows:

$$D_{\bar{F}_i}(u) = \frac{1}{L-1}\sum_{j \neq i}(F_{ij}(u) - \bar{F}_i(u)) \cdot (F_{ij}(u) - \bar{F}_i(u))^T, \quad (10)$$

where F_{ij} is the deformation function that warps T_i to T_j. The covariance matrix, defined at each pixel u, is a measure of the variability associated with the estimated deformation functions. Two choices of pixel-wise measures of variability are given by 1) the determinant, $\phi(D_{\bar{F}_i}(u)) = |D_{\bar{F}_i}(u)|$, and 2) the trace, $\phi(D_{\bar{F}_i}(u)) = \mathrm{tr}(D_{\bar{F}_i}(u))$. Pixels with large (small) values of ϕ indicate high (low) variability in the deformations F_{ij}. We propose using the values of ϕ to determine the optimal model for a given finger. We define the ith index of deformation, Φ_i, as

$$\Phi_i = \frac{1}{|S|}\sum_{u=1}^{|S|} \phi(D_{\bar{F}_i(u)}), \quad (11)$$

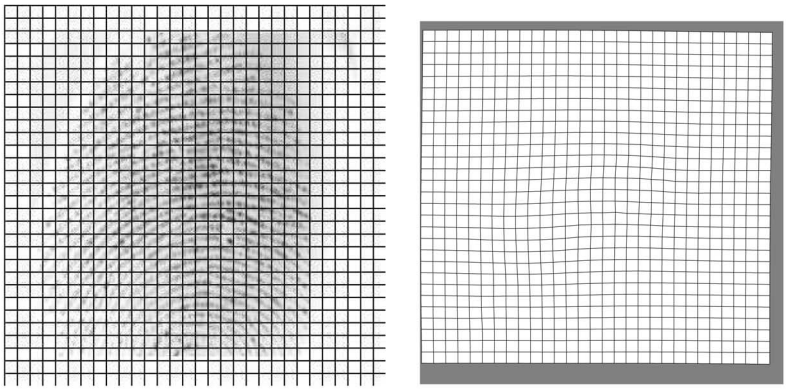

(d)

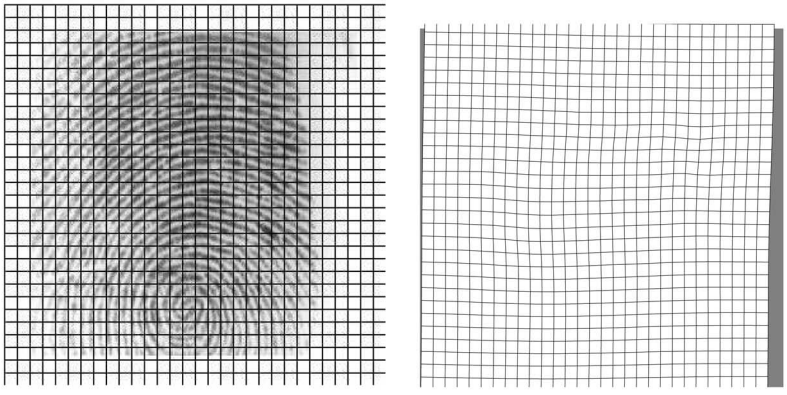

(e)

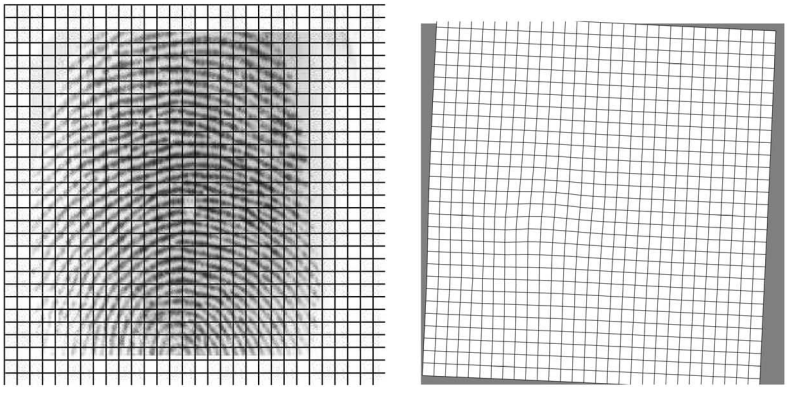

(f)

Fig. 6b. (continued). (d) $\Phi = 83.12$. (e) $\Phi = 94.34$. (f) $\Phi = 232.53$.

where $\phi(D) = tr(D)$ and $|S|$ is the number of pixels in the domain S. Subsequently, we choose T_{i^*} as the template with the smallest variability in deformation if $i^* = \arg\min_i \Phi_i$. In effect, we choose that template T_i that minimizes the average variation across pixels measured in terms of Φ_i. Low (high) values of the index of deformation indicate that the warping functions are similar (dissimilar) to each other.

3.2 Eliminating Erroneous Correspondences

For each baseline fingerprint impression, it is important to determine the set of minutiae points that are correctly paired to form a correspondence. The average deformation model is sensitive to the accuracy of the ridge curve correspondence, which, in turn, depends on the minutiae correspondence. It is, therefore, necessary to check the correctness of the minutiae correspondences prior to obtaining the ridge curve correspondences. Fig. 8a presents an example of two incorrect minutiae correspondences which result in incorrect ridge curve correspondences (Fig. 8b). These erroneous correspondences have to be eliminated prior to computing the average deformation model; failure to exclude such minutiae points results in a warping model exhibiting spurious distortions.

For the given baseline fingerprint impression, minutiae points that have a correspondence with at least ℓ ($\ell = 5$) of the remaining $L - 1$ impressions are extracted. We denote the set of all such minutiae points by

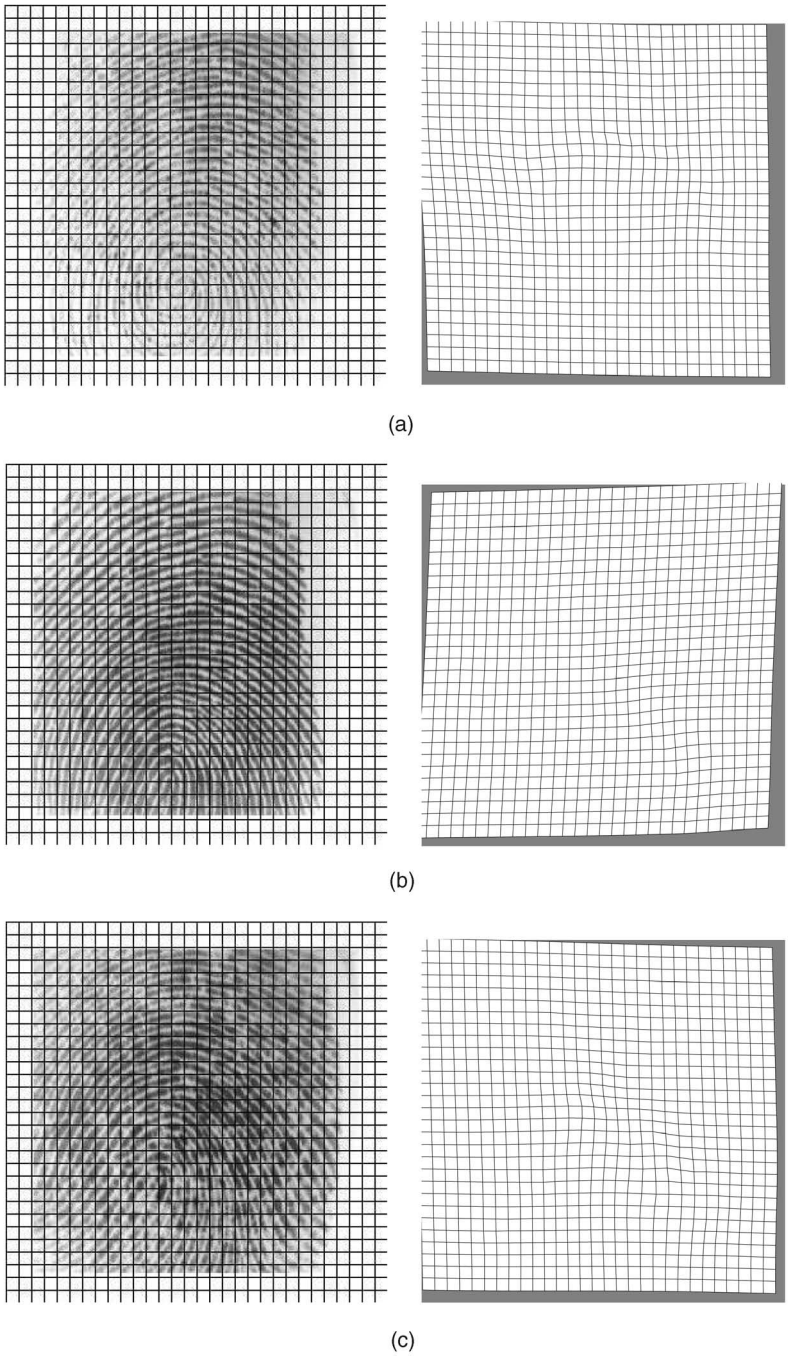

Fig. 7. The average deformation model (shown as deformations on a reference grid) of three different fingers. (a) $\Phi = 46.68$. (b) $\Phi = 37.59$. (c) $\Phi = 85.18$.

$M = \{m_i,\ i = 1, 2, \ldots, K\}$. Each m_i has a corresponding minutiae point in at least ℓ of the $L-1$ impressions. We denote these pairings by $(m_i, p_1), (m_i, p_2), \ldots, (m_i, p_{\ell_i})$, where ℓ_i is the total number of pairings. We next develop a measure of reliability for minutiae point m_i as follows:

1. Sampled ridge point correspondences are obtained for each (m_i, p_j), $j = 1, 2, \ldots, n_i$, based on which a TPS deformation model, $F_{(m_i,p_j)}$ is computed. The average deformation model for the minutiae point m_i is given by

$$\bar{F}_{m_i}(u) = \frac{1}{\ell_i}\sum_{j=1}^{\ell_i} F_{(m_i,p_j)}(u).$$

   Here, the average deformation model is obtained in a 10×10 square region, say S_{m_i}, centered at m_i.

2. Let

$$D_{\bar{F}_{m_i}}(u) = \frac{1}{\ell_i}\sum_{j=1}^{\ell_i}(F_{(m_i,p_j)}(u) - \bar{F}_{m_i}(u)) \cdot (F_{(m_i,p_j)}(u) - \bar{F}_{m_i}(u))^T \quad (12)$$

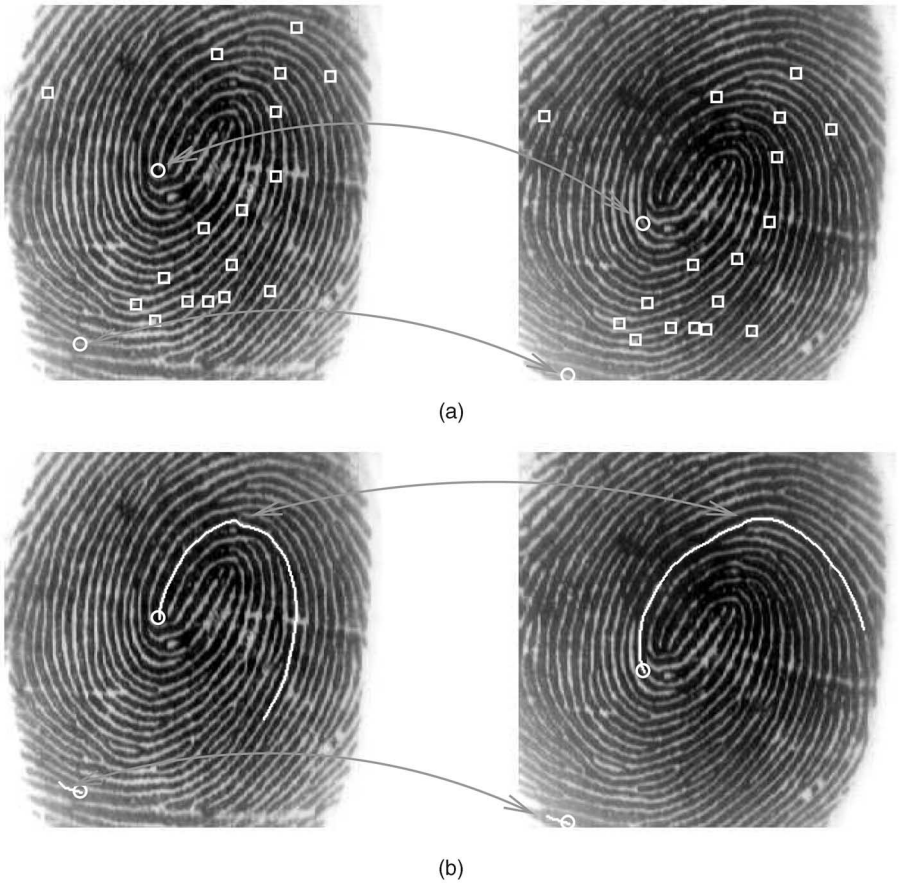

Fig. 8. (a) Examples of incorrect minutiae correspondences. (b) These result in erroneous ridge curve correspondences.

denote the site-wise variability measure of the deformations $F_{(m_i,p_j)}$ around $\bar{F}_{m_i}$. The average variability is measured by

$$R_{m_i} = \frac{1}{|S_{m_i}|} \sum_{u=1}^{|S_{m_i}|} \text{trace}(D_{\bar{F}_{m_i}}(u))$$

with small values of R_{m_i} indicating better reliability. Correspondences pertaining to those minutiae points with R_{m_i} values lower than the pth percentile (e.g., $p = 60$) are used to develop the average deformation model for the template fingerprint.

For the incorrect minutiae correspondences in Fig. 8, the value of R for the top minutiae point was 93.2 (the sixtieth percentile value of R was 55.5 for this template), while the lower minutiae point occurred in less than five corresponding pairs and was, therefore, eliminated. Fig. 9a shows the average deformation model that results for this template when all correspondences are used (i.e., $p = 100$); Fig. 9b gives the deformation model for $p = 60$.

4 Experimental Results

In order to apply the TPS model to reliably estimate fingerprint deformation, we need to have several impressions of the same finger. Large number of impressions of a finger are not available in standard fingerprint databases (e.g., FVC 2002 [30]). Therefore, fingerprint images of 50 fingers (corresponding to five subjects) were acquired using the Identix sensor (256×255, 380 dpi) over a period of two weeks in our lab. The subjects did not deliberately distort their fingerprints while interacting with the sensor. There were 32 impressions corresponding to every finger, resulting in a total of 1,600 impressions. One half of the impressions ($L = 16$ for each finger, resulting in 800 impressions) were used as templates to compute the average deformation model for each finger, while the remaining 800 impressions were used as query images for testing. For each template image, T, the minutiae set, M_T, and the thinned image, R_T, were extracted (Fig. 10). The average deformation model of T, $\bar{F}_T$, was obtained based on pairings with the remaining 15 impressions of the same finger ((7) with $\lambda = 0.1$). The minutiae set M_T was transformed to the deformed set, $MD_T \equiv \bar{F}_T(M_T)$ using $\bar{F}_T$. A total of 800 sets (50×16) of deformed minutiae points were thus obtained. In order to test the matching performance of the deformed minutiae sets and the utility of the index of deformation, Φ, the following two experiments were conducted. In both these experiments, the minutiae matcher described in [29] was used to generate the matching (similarity) score.

In the first experiment, the matching performance using the average deformation model was evaluated. Every template image, T, was compared with every query image, Q, and two types of matching scores were generated for each comparison: the matching score obtained by matching 1) M_T with M_Q and 2) MD_T with M_Q. The Receiver Operating Characteristic (ROC) curve plotting the genuine accept rate (GAR) against the false accept rate (FAR) at various matching thresholds is presented in Fig. 11. An

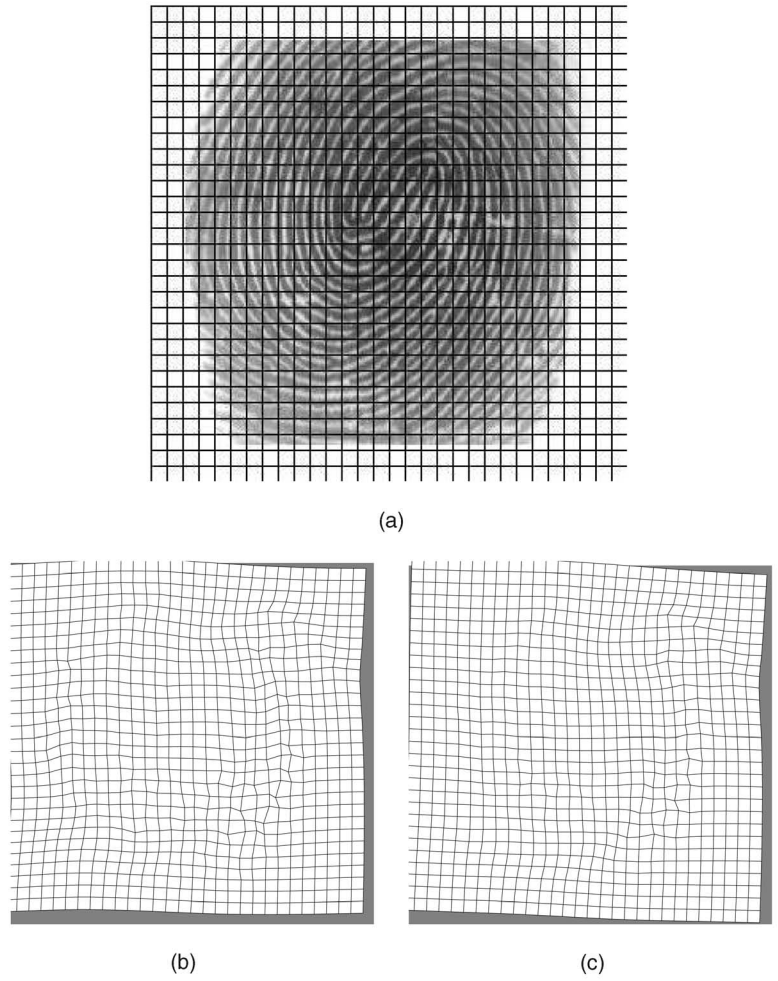

Fig. 9. Effect of eliminating unreliable minutiae correspondences on the average deformation model. (a) Template fingerprint, (b) average deformation model with $p = 100$, $\Phi = 102.16$, and (c) average deformation model with $p = 60$, $\Phi = 67.78$.

overall improvement is observed when the average deformation model is used to distort M_T prior to matching.

In the second experiment, the advantage of using the index of deformation is demonstrated. The Φ-index of deformation (with $\phi(D) = \mathrm{tr}(D)$) of every template image is used to rank the templates according to their variability in the distortion. The template images can now be split into two sets: 1) impressions with the least Φ values for every finger (the Φ-optimal templates) and 2) the remaining impressions for every finger (the Φ-suboptimal templates). We repeated the matching procedure outlined above using these two template sets. The resulting ROC curve is shown in Fig. 12. From the figure, it is clear that using Φ-optimal templates results in better performance compared to using Φ-suboptimal templates. Further, the Φ-suboptimal templates still yield better performance compared to the nondistorted templates, thus demonstrating the importance of the average deformable model.

The registration between the query and the template minutiae sets is significantly improved when the average deformation model based on ridge curves is applied prior to the rigid transformation. The improved registration allows our minutiae matcher to specify stricter bounding boxes when the query and deformed template minutiae points are compared without compromising the genuine matching scores. The added advantage of specifying stricter bounding boxes is that the number of false accepts is highly reduced resulting in a better ROC curve.

5 Summary and Future Work

In this paper, we have developed a deformation model for estimating the distortion effects in fingerprint impressions based on ridge curve correspondence. The proposed model was observed to result in a better performance compared to a model based on minutiae pattern correspondence. Our warping model samples the ridge curve and uses thin-plate splines for estimating the nonlinear deformation. The average deformation model of a finger is a compact description of the intraclass variability due to nonlinear distortions. We have also proposed an index of deformation, Φ, for selecting the optimal average deformation model corresponding to a finger by minimizing distortion variability. It was shown that the Φ-optimal deformation models result in superior matching performance compared to Φ-suboptimal models.

The subjects did not consciously distort their fingerprints when interacting with the sensor and, hence, one cannot predict the nature of the distortions present in the acquired images before hand. The significance of the proposed technique is its ability to compare multiple impressions of

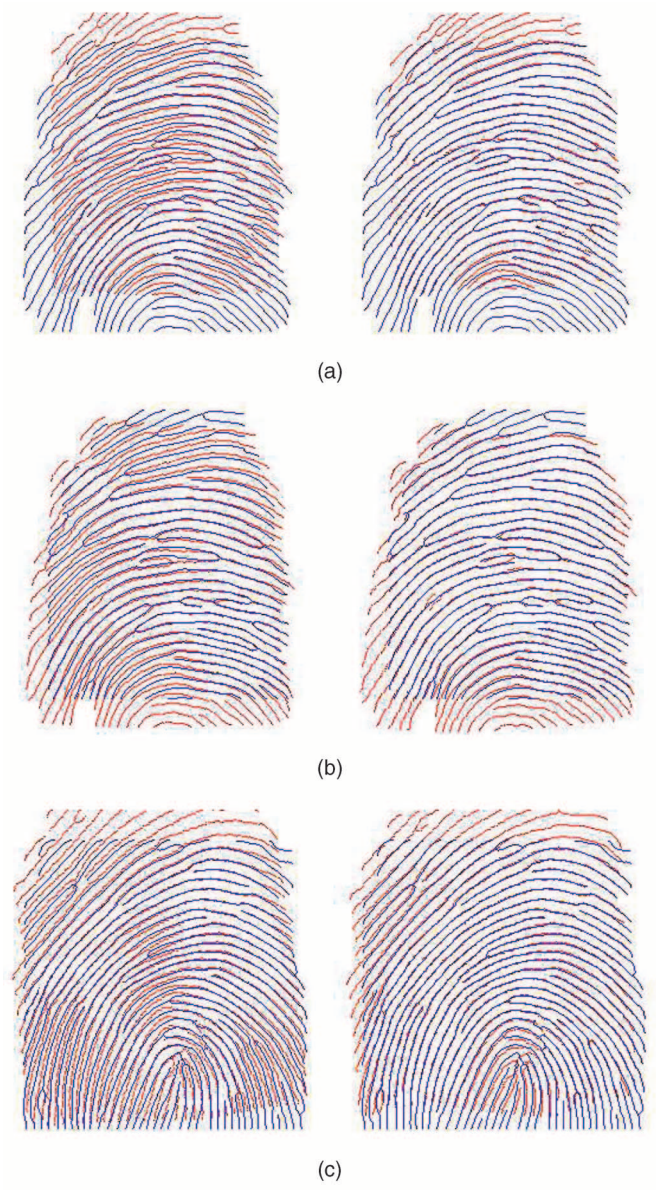

Fig. 10. Improved alignment of template and query images using ridge curve correspondences (right panel). The alignment using minutiae correspondences is shown in the left panel. Both sets of alignment use the TPS warping model.

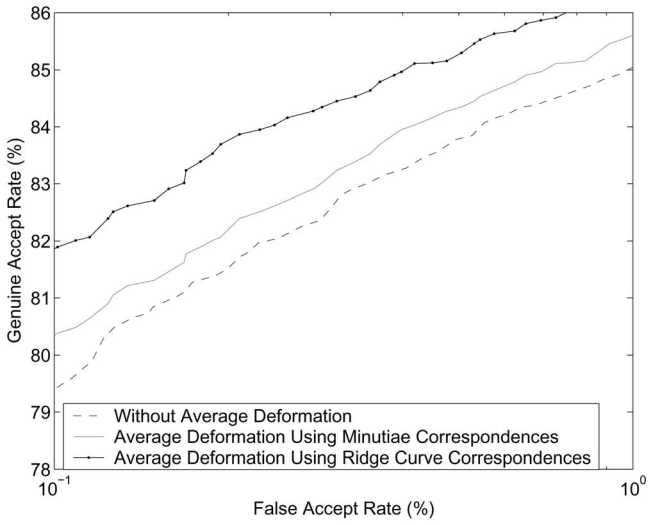

Fig. 11. Improvement in matching performance when ridge curve correspondences is used to develop the average deformation model.

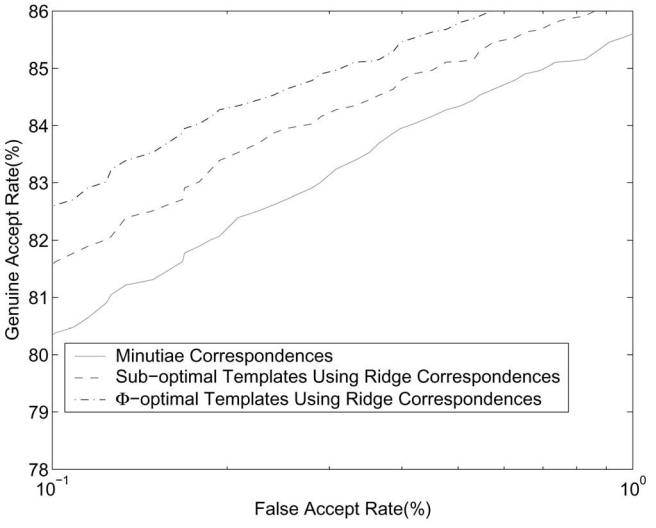

Fig. 12. Matching performance when the Φ index of deformation is used to select optimal templates. Both optimal and suboptimal templates using ridge curve correspondences result in superior matching performance compared to minutiae correspondences.

a finger with a baseline impression, thereby determining the nonlinear average distortion automatically. However, the accuracy of the technique is largely defined by the reliability of minutiae point correspondences generated by the algorithm. Therefore, excessive deformations may result in erroneous minutiae (and ridge) correspondences confounding the average deformation model. Furthermore, the proposed model assumes that the elastic nature of the skin can be approximated using thin-plate splines. It may be instructive to use alternate models based on the Navier-Stokes equation in order to describe the deformation [31].

Future work includes developing an incremental approach to updating the average deformation model, i.e., updating the current average deformation model of a finger by using information presented by newly acquired fingerprint impressions. We have used a simple pixel-wise averaging measure to compute the average deformation model in this paper. This measure is sensitive to extreme deformations born out by outliers; thus, we seek more robust measures of describing the finger specific average deformation model. We are also working on developing ridge curve correspondences between pairs of fingerprint impressions by viewing the thinned images solely as a set of curves in R^2.

Acknowledgments

A preliminary version of this work appeared in [1].

References

[1] A. Ross, S.C. Dass, and A.K. Jain, "Estimating Fingerprint Deformation," *Proc. Int'l Conf. Biometric Authentication*, pp. 249-255, July 2004.

[2] A.M. Bazen, G.T.B. Verwaaijen, S.H. Gerez, L.P.J. Veelenturf, and B.J. van der Zwaag, "A Correlation-Based Fingerprint Verification System," *Proc. ProRISC2000 Workshop Circuits, Systems, and Signal Processing*, Nov. 2000.

[3] D. Roberge, C. Soutar, and B. Vijaya Kumar, "High-Speed Fingerprint Verification Using an Optical Correlator," *Proc. SPIE,* vol. 3386, pp. 123-133, 1998.
[4] Z.M. Kovács-Vajna, "A Fingerprint Verification System Based on Triangular Matching and Dynamic Time Warping," *IEEE Trans. Pattern Analysis and Machine Intelligence,* vol. 22, no. 11, pp. 1266-1276, Nov. 2000.
[5] D. Maio and D. Maltoni, "Direct Gray-Scale Minutiae Detection in Fingerprints," *IEEE Trans. Pattern Analysis and Machine Intelligence,* vol. 19, no. 1, pp. 27-40, Jan. 1997.
[6] N.K. Ratha and R.M. Bolle, "Effect of Controlled Acquisition on Fingerprint Matching," *Proc. Int'l Conf. Pattern Recognition,* vol. 2, pp. 1659-1661, 1998.
[7] C. Dorai, N. Ratha, and R. Bolle, "Detecting Dynamic Behavior in Compressed Fingerprint Videos: Distortion," *Proc. Computer Vision and Pattern Recognition,* pp. 320-326, June 2000.
[8] L.R. Thebaud, "Systems and Methods with Identity Verification by Comparison and Interpretation of Skin Patterns such as Fingerprints," US Patent 5,909,501, 1999.
[9] A.M. Bazen and S. Gerez, "Fingerprint Matching by Thin-Plate Spline Modeling of Elastic Deformations," *Pattern Recognition,* vol. 36, no. 8, pp. 1859-1867, Aug. 2003.
[10] A. Senior and R. Bolle, "Improved Fingerprint Matching by Distortion Removal," *IEICE Trans. Information and Systems,* vol. 84, no. 7, pp. 825-831, july 2001.
[11] C. Watson, P. Grother, and D. Cassasent, "Distortion-Tolerant Filter for Elastic-Distorted Fingerprint Matching," *Proc. SPIE Optical Pattern Recognition,* pp. 166-174, 2000.
[12] R. Cappelli, D. Maio, and D. Maltoni, "Modelling Plastic Distortion in Fingerprint Images," *Proc. Second Int'l Conf. Advances in Pattern Recognition,* Mar. 2001.
[13] R. Cappelli, R. Erol, D. Maio, and D. Maltoni, "Synthetic Fingerprint-Image Generation," *Proc. 15th Int'l Conf. Pattern Recognition,* vol. 3, Sept. 2000.
[14] A. Almansa and L. Cohen, "Fingerprint Image Matching by Minimization of a Thin-Plate Energy Using a Two-Step Algorithm with Auxiliary Variables," *Proc. IEEE Workshop Application of Computer Vision,* pp. 35-40, Dec. 2000.
[15] A. Ross, S.C. Dass, and A.K. Jain, "A Deformable Model for Fingerprint Matching," *Pattern Recognition,* vol. 38, no. 1, pp. 95-103, Jan. 2005.
[16] D.J. Burr, "A dynamic Model for Image Registration," *Computer Graphics and Image Processing,* vol. 15, pp. 102-112, 1981.
[17] L. Younes, "Optimal Matching between Shapes via Elastic Deformations," *Image and Vision Computing,* vol. 17, pp. 381-389, 1999.
[18] J.L. Barron, D.J. Fleet, and S.S. Beauchemin, "Performance of Optical Flow Techniques," *Int'l J. Computer Vision,* vol. 12, pp. 43-77, 1994.
[19] G.E. Christensen, R.D. Rabbitt, and M.I. Miller, "Deformable Templates Using Large Deformation Kinetics," *IEEE Trans. Image Processing,* vol. 5, pp. 1435-1447, 1996.
[20] S.C. Joshi and M.I. Miller, "Landmark Matching via Large Deformation Diffeomorphisms," *IEEE Trans. Image Processing,* vol. 9, pp. 1357-1370, 2000.
[21] Y. Amit, U. Grenander, and M. Piccioni, "Structural Image Restoration through Deformable Templates," *J. Am. Statistical Assoc.,* vol. 86, pp. 376-387, 1991.
[22] J.M. Cartensen, "An Active Lattice Model in a Bayesian Framework," *Computer Vision and Image Understanding,* vol. 63, no. 2, pp. 380-387, 1996.
[23] C.A. Glasbey and K.V. Mardia, "A Penalized Likelihood Approach to Image Warping," *J. Royal Statistical Soc., Series B, Statistical Methodology,* vol. 63, no. 3, pp. 465-514, 2001.
[24] F.L. Bookstein, "Principal Warps: Thin-Plate Splines and the Decomposition of Deformations," *IEEE Trans. Pattern Analysis and Machine Intelligence* vol. 11, pp. 567-585, 1989.
[25] K.V. Mardia and T.J. Hainsworth, "Image Warping and Bayesian Reconstruction with Gray-Level Templates," *Statistics and Images: Volume 1,* K.V. Mardia and G.K. Kanji, eds., Oxford: Carfax, pp. 257-280, 1993.
[26] K.V. Mardia, T.J. Hainsworth, and J.F. Haddon, "Deformable Templates in Image Sequences," *Proc. Int'l Conf. Pattern Recognition,* pp. 132-135, 1992.
[27] I.L. Dryden and K.V. Mardia, *Statistical Shape Analysis.* John Wiley and Sons, 1998.
[28] F.L. Bookstein, "Landmark Methods for Forms without Landmarks," *Medical Image Analysis,* vol. 1, pp. 225-243, 1997.
[29] A.K. Jain, L. Hong, and R. Bolle, "Online Fingerprint Verification," *IEEE Trans. Pattern Analysis and Machine Intelligence,* vol. 19, no. 4, pp. 302-314, Apr. 1997.
[30] D. Maio, D. Maltoni, R. Cappelli, J.L. Wayman, and A.K. Jain, "FVC2002: Fingerprint Verification Competition," *Proc. Int'l Conf. Pattern Recognition,* pp. 744-747, Aug. 2002.
[31] S. Novikov and O. Ushmaev, "Registration and Modeling of Elastic Deformations of Fingerprints," *Proc. Int'l ECCV Workshop Biometric Authentication,* pp. 80-88, May 2004.

Arun Ross received the BE (Hons.) degree in computer science from the Birla Institute of Technology and Science, Pilani, India, in 1996. He received the MS and PhD degrees in computer science and engineering from Michigan State University in 1999 and 2003, respectively. He is an assistant professor in the Lane Department of Computer Science and Electrical Engineering at West Virginia University. Between July 1996 and December 1997, he worked with the Design and Development Group of Tata Elxsi (India) Ltd. in Bangalore. He also spent three summers (2000-2002) with the Imaging and Visualization Group at Siemens Corporate Research, Inc., Princeton, New Jersey working on fingerprint recognition algorithms. His research interests include multimodal biometrics, fingerprint/iris analysis, and statistical pattern recognition. He is a member of the IEEE.

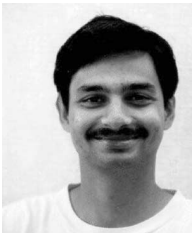

Sarat C. Dass received the MSc degree and the PhD degree in statistics from Purdue University in 1995 and 1998, respectively. He worked as a visiting assistant professor (in the period 1998-2000) in the Department of Statistics, University of Michigan. Starting in 2000, he joined the Department of Statistics and Probability at Michigan State University. His research and teaching interests include statistical image processing and pattern recognition, shape analysis, spatial statistics, Bayesian computational methods, foundations of statistics, and nonparametric statistical methods. He has been actively collaborating with computer scientists in several pattern recognition and image processing problems.

Anil K. Jain received the BTech degree from the Indian Institute of Technology, Kanpur, in 1969 and the MS and PhD degrees from The Ohio State University in 1970 and 1973, respectively. He is a university distinguished professor in the Department of Computer Science and Engineering at Michigan State University. His research interests include statistical pattern recognition, data clustering, texture analysis, document image understanding, and biometric authentication. He has received a Fulbright Research Award, a Guggenheim fellowship, and the Alexander von Humboldt Research Award. He delivered the 2002 Pierre Devijver lecture sponsored by the International Association of Pattern Recognition (IAPR) and received the 2003 IEEE Computer Society Technical Achievement Award. He holds six patents in the area of fingerprint matching and is the author of a number of books including *Handbook of Face Recognition* (Springer, 2005), *Handbook of Fingerprint Recognition* (Springer, 2003) (received the PSP award from the Association of American Publishers), and *BIOMETRICS: Personal Identification in Networked Society* (Kluwer, 1999). He is a fellow of the AAAS, ACM, IAPR, and IEEE.